



Evaluating the Use of Multisite Probabilistic Seismic Hazard Analysis: A Case of Sarpol-e Zahab City, Iran

SAMAN YAGHMAEI-SABEGH¹ and AMIRREZA MOHAMMADI¹

Abstract—This paper evaluates the use of multisite (MS) probabilistic seismic hazard analysis (PSHA), which estimates the annual exceedance rate of a given level of ground motion in at least one of several sites as one of several possible results. For this purpose, (1) MS-PSHA is implemented through the Monte Carlo approach, taking into account various area sizes and correlation distances (*CDs*), and then (2) two proposals are represented as applications of MS-PSHA outcomes, both with reference to Sarpol-e Zahab City, a seismically active region located in the west of Iran. The first proposal attempts to determine the current code design probability of exceedance in at least one site, and the second one defines collapse prevention levels based on different probabilities of exceedance in at least one site. The efficiency of the results is discussed mainly by comparing them to recorded peak ground accelerations (PGAs) of three earthquakes, including the 2017 Sarpol-e Zahab 7.3 M_w event that largely exceeded the code design spectrum. MS-PSHA results demonstrate reasonable performance both in determining design ground motions and evaluating current design code when the exact seismic parameters of the study area are used in the analysis. Moreover, developed code-type design spectra based on MS-PSHA provided safety against collapse compared to a recently occurring low-probability event. MS estimates for various *CDs* and probabilities of exceedance in at least one site can also provide flexible design strategies regarding the importance of a structure and expected damage on a regional scale.

Keywords: Multisite probabilistic seismic hazard analysis, correlation between ground motions, design spectrum, Sarpol-e Zahab earthquake.

1. Introduction

Despite defining design acceleration based on probabilistic seismic hazard analysis (PSHA), widespread failures due to large earthquakes have still been observed regardless of building construction

defects. In strong-motion stations near the seismic sources, the estimated ground motions are frequently not comparable with recorded ones (e.g., 2017 Sarpol-e Zahab 7.3 M_w earthquake, six events were reported by Zuccolo et al. (2011)). Even though PSHA is still used as a practical tool and provides valuable information, there are discussions about its weaknesses (Albareello & D'amico, 2008; Frankel, 2013; Hanks et al., 2012; Iervolino, 2013; Klüge, 2012; Kossobokov & Nekrasova, 2012; Panza et al., 2011, 2014; Stein et al., 2011; Stirling, 2012; Wyss, 2015; Wyss & Rosset, 2013).

Based on arguments about discarding PSHA because of its weaknesses (e.g., Geller, 2011) and, on the other hand, accepting it as a reliable tool after addressing its weaknesses (Anderson & Biasi, 2016; Frankel, 2013; Hanks et al., 2012; Stirling, 2012; Wong, 2014), there is a need to perform a complementary, or alternative, hazard analysis in situations where (1) conventional analysis outcomes (e.g., the design spectrum) have been largely and frequently exceeded, and (2) it is necessary to account for correlation between ground motions in different sites over a region. In this context, Iervolino (2013) proposed a new concept named regional hazard. He believed that ground motions estimated based on this method could be compared to recorded ground motions in epicentral areas, as well as to assign design acceleration in high-importance areas. To address comparison issues and considering the high probability of design acceleration exceedance in epicentral areas, he suggested accounting for a level of ground motion with a specific annual frequency exceedance in at least one site of several sites in the area (Iervolino, 2013).

¹ Department of Civil Engineering, University of Tabriz, Tabriz, Iran. E-mail: s_yaghmaei@tabrizu.ac.ir

Sokolov and Wenzel (2015) considered combining two concepts as multiple-location probabilistic seismic hazard assessments. These two concepts are (1) the level of ground motion with a specific annual rate of exceedance in at least one site of several sites and (2) the level of ground motion with a specific annual rate of simultaneous exceedance in all sites. They performed this analysis for zones of varying sizes and correlation levels.

Giorgio and Iervolino (2016) proposed a probabilistic framework for multisite probabilistic seismic hazard analysis (MS-PSHA) that, by dealing with dependence between exceedance counting processes originating from the correlation between ground motion parameters in multiple sites, estimates the probability of several exceedances from ground motion thresholds in multiple sites, as well as the probability of the total number of exceedances in an arbitrary time interval in all proposed sites, which is beneficial for hazard validation studies; see, for example, Schorlemmer et al. (2007), Albarello and D'Amico (2008), and Iervolino et al. (2017).

To evaluate the MS-PSHA performance, Sokolov et al. (2016) compared the MS estimates with ground motions of two destructive earthquakes, i.e., 1996 Chi-Chi and 2008 Wenchuan. In their work, MS-PSHA was implemented for zones with different sizes and levels of correlation by considering the within- and between-earthquake correlation of residuals and using a creative approach for calculating frequency exceedance rates. Compared to recorded ground motions, they showed that MS-PSHA made a more reasonable evaluation than the single-site one.

Regarding MS-PSHA, previous studies have yielded hazard curves based on specific characteristics or a set of probabilities mostly related to the exceedance of ground motion thresholds in different sites. The current study, besides implementing MS-PSHA for the seismically active city of Sarpol-e Zahab, offers two proposals on the use of MS-PSHA: (1) as a probabilistic measure to evaluate the current code design spectrum from a social perspective (i.e., its exceedance probability in at least one site), and (2) as a tool to define the collapse prevention level and different possible design strategies with respect to correlation distance (*CD*) and exceedance probability in at least one site. This study performs MS-PSHA

for Sarpol-e Zahab City based on statistical concepts by simulating a long-duration seismic catalog through the Monte Carlo technique. For each earthquake in the catalog, the required parameters are selected randomly with respect to their distributions. The preliminary output of the analysis is MS hazard curves and estimated MS-PGAs with a return period of 475 years for three areas of different sizes. The outputs of the proposed applications are (1) exceedance probability of Iranian code design spectrum in at least one site of several in Sarpol-e Zahab City and (2) adopted maximum considered earthquake (MCE) ground motions using MS-PSHA estimates and developed design-based earthquake (DBE)-level uniform hazard spectra.

Following a review of fundamental concepts in Sect. 2 of this paper, Sect. 3 explains the studied area of interest for MS-PSHA and input parameters. It should be noted that in this section, the MS-PSHA analysis is implemented for Sarpol-e Zahab City in western Iran by defining three zones with different areas. Section 4 evaluates the efficiency of the estimates by comparing them to recorded ground motions. Section 5 suggests two additional applications of MS-PSHA results. Section 6 presents extended examples based on proposals with reference to Sarpol-e Zahab City and investigates their performance regarding a recently recorded low-probability event. Sections 7 and 8 provide a further explanation for using *CD* for different purposes and conclusions, respectively.

2. Multisite Probabilistic Seismic Hazard Analysis

Conventional PSHA estimates the annual exceedance rate from specific levels of ground motion parameters (Cornell, 1968). Exceedance rates for one site affected by one seismic source can be estimated from Eq. (1) after preliminary steps:

$$\lambda(Y > y_i) = \nu \int_{M_{\min}}^{M_{\max}} \int_0^{r_{\max}} P(Y > y_i | M, R) f_M(m) f_R(r) dr dm, \quad (1)$$

where $P(Y > y_i | M, R)$ denotes the probability of exceedance from ground motion level y_i for a given

magnitude M and distance from source R , and v is the rate of earthquake occurrence greater than M_{\min} from the source. M_{\max} and M_{\min} are the maximum and minimum earthquake magnitudes that each source can produce, respectively, and r_{\max} is the maximum distance of the site from the source. The probability distributions of magnitude and distance are denoted by $f_M(m)$ and $f_R(r)$, respectively. One of the key concepts in the seismic hazard analysis of a region that must be applied correctly is the correlation of ground motion parameters at different sites (Esposito & Iervolino, 2012; Goda & Hong, 2008; Jayaram & Baker, 2009; Park et al., 2007; Rhoades & McVerry, 2001; Sokolov & Wenzel, 2011; Wesson & Perkins, 2001). Therefore, in the following section, the components of correlation between ground motions are defined, followed by a description of how to model them in MS-PSHA.

2.1. Identifying and Modeling the Ground Motion Parameter Correlation

Ground motion parameters that distribute log normally at site m due to earthquake n are predicted by ground motion prediction equations (GMPEs) of the form:

$$\ln(Y_{m,n}) = \ln(\bar{Y}_{m,n}) + \varepsilon_{m,n} + \eta_n, \quad (2)$$

where $Y_{m,n}$ denotes ground motion parameters (e.g., peak ground acceleration [PGA]); $\ln(\bar{Y}_{m,n})$ is the median ground motion predicted by GMPEs according to parameters such as magnitude M , distance from source R , type of fault, and local site conditions. $\varepsilon_{m,n}$ and η_n denote the within-earthquake and between-earthquake residuals that are independent random variables with zero mean and standard deviation of σ_ε and σ_η , respectively. The total variance σ_T^2 is equal to $\sigma_T^2 = \sigma_\varepsilon^2 + \sigma_\eta^2$.

The correlation among between-earthquake residuals (between-earthquake correlation) and within-earthquake residuals (within-earthquake correlation) is the primary source of correlation between ground motion parameters (Jayaram & Baker, 2008; Park et al., 2007; Sokolov & Wenzel, 2011). In the following, the correlation structure of between-earthquake residuals and within-earthquake residuals is characterized.

Using the correlation coefficient definition and assuming that the covariance of between-earthquake residuals is equal to their variance (σ_η^2), the between-earthquake correlation coefficient is given by Eq. (3) (Sokolov & Wenzel, 2011; Wesson & Perkins, 2001):

$$\rho_\eta = \frac{\sigma_\eta^2}{\sigma_\eta^2 + \sigma_\varepsilon^2} = \frac{\sigma_\eta^2}{\sigma_T^2}. \quad (3)$$

Using geostatistical tools and basic models, the within-earthquake correlation coefficient could be estimated. Some of these models include exponential and Gaussian models, with the exponential model being chosen for this study due to its extensive application (Jayaram & Baker, 2009). The exponential correlation model, which estimates the within-earthquake correlation coefficient in sites with a separation distance h , is defined as follows:

$$\rho_\varepsilon(h) = e^{ah^b}, \quad (4)$$

in which $\rho_\varepsilon(h) = \rho_{\varepsilon_{m,n,1}, \varepsilon_{m,n,2}}$ is the empirical within-earthquake correlation coefficient calculated for residuals at two sites with a distance of h ; a and b are statistically constant coefficients. The CD parameter could be used to describe the level of within-earthquake correlation (Wang & Takada, 2005). This parameter refers to the distance between two sites at which the within-earthquake correlation coefficient ρ_ε equals 0.368. Lower CD implies a high variability of ground motions in different sites; however, higher CD implies a linear distribution of ground motions.

$$\rho_T(h) = \frac{\sigma_\eta^2 + \rho_\varepsilon(h)\sigma_\varepsilon^2}{\sigma_T^2} = \rho_\eta + \rho_\varepsilon(h) \left(\frac{\sigma_\varepsilon^2}{\sigma_T^2} \right). \quad (5)$$

The total correlation coefficient $\rho_T(h)$, which contains two components of correlation, can be calculated as follows (Sokolov & Wenzel, 2011):

Using the previously described correlation structure of residuals, we need to generate correlated residuals to acquire correlated ground motions. For this purpose, the following steps should be taken by assuming that the distribution of ground motion parameters by GMPEs at the sites $j = 1, 2, \dots, f$ is not marginal normal but joint normal (Park et al., 2007): (1) defining the correlation matrix, which implies the level of correlation between the sites using Eq. (6); (2) generating a vector of independent standard

normal random variables $U = [U_1, U_2, \dots, U_f]$ with a standard deviation of σ_T ; (3) applying the Cholesky decomposition to the correlation matrix to divide it into a product of two matrices $\Sigma = CC^T$; and finally, (4) multiplying the lower rectangular matrix of C , obtained from the correlation matrix decomposition, by generated vector U to obtain the correlated residuals. Now, by adding these correlated residuals to $\ln(\bar{Y}_{m,n})$, the correlated ground motion parameters will be obtained. As it can be seen in Eq. (6), the correlation matrix consists of two terms: the first determines the correlation between inter-event residuals, which are perfectly and positively correlated at all sites in one event and could be modeled by Eq. (3), and the second determines the correlation between intra-event residuals, using an empirical correlation model [e.g., Eq. (4)].

$$\Sigma = \frac{\sigma_\eta^2}{\sigma_T^2} \begin{bmatrix} 1 & 1 & \dots & 1 \\ 1 & 1 & \vdots & 1 \\ \vdots & \vdots & \ddots & \vdots \\ 1 & 1 & \dots & 1 \end{bmatrix} + \frac{\sigma_\varepsilon^2}{\sigma_T^2} \begin{bmatrix} 1 & \rho_{\varepsilon_{1,2}} & \dots & \rho_{\varepsilon_{1,f}} \\ \rho_{\varepsilon_{2,1}} & 1 & \vdots & \rho_{\varepsilon_{2,f}} \\ \vdots & \vdots & \ddots & \vdots \\ \rho_{\varepsilon_{f,1}} & \rho_{\varepsilon_{f,2}} & \dots & 1 \end{bmatrix}. \quad (6)$$

2.2. Implementing the Monte Carlo Technique

Using adequate data, including all possible seismic events over a long period of time, could be a challenge in hazard analysis. This study applies the Monte Carlo technique to consider the random combination of input parameters and the excessive repetition of the simulation process. A long-duration catalog compatible with each source zone's seismic data is generated based on this technique. This method has been used successfully in several research projects (Assatourians & Atkinson, 2013; Bourne et al., 2015; Ebel & Kafka, 1999; Musson, 1999; Sokolov & Wenzel, 2011; Weatherill & Burton, 2010; Chioccarelli et al., 2019).

The procedure for generating the current study catalog is as follows: the coordinates of each event inside the corresponding zone are selected randomly with the assumption that coordinates are distributed

uniformly throughout the seismic zone. The depth of each event is randomly selected from the zone-based depth distribution, and the magnitude of each event is randomly selected from the frequency-magnitude distribution of that seismic zone (Sokolov & Wenzel, 2011). Eventually, this technique yields a comprehensive catalog that takes into account all possible seismic events.

Now, by identifying and applying the correlation between ground motion parameters of the prepared catalog, the most crucial part of MS-PSHA is performed; in the following, the annual exceedance rates of specific levels in at least one site are simply estimated by statistical concepts. To estimate the annual exceedance rate of a specific level of ground motion y_i in one single site, the number of exceedances from the level y_i could be divided by the total duration (T_{tot}) of catalog used ($\lambda_i(Y > y_i) = N(Y > y_i)/T_{\text{tot}}$). To implement this into MS-PSHA, each earthquake's maximum produced ground motion is selected, considering all sites. Then, by repeating this procedure for all earthquakes of the catalog, a set of maximum ground motions is obtained (Y_{max}). Now, the annual exceedance rate of a specific level of ground motion y_i in at least one site ($\lambda_{i,\text{one}}(Y_{\text{max}} > y_i)$) could be estimated from the obtained set (Y_{max}) by Eq. (7) (Sokolov & Ismail-Zadeh, 2016):

$$\lambda_{i,\text{one}}(Y_{\text{max}} > y_i) = \frac{N_{i,\text{one}}(Y_{\text{max}} > y_i)}{T_{\text{tot}}}, \quad (7)$$

where $N_{i,\text{one}}(Y_{\text{max}} > y_i)$ is the number of exceedances from the level y_i in the obtained set (Y_{max}).

Figure 1 shows how to implement MS-PSHA in three steps. The first step of this flowchart specifies various inputs and parameters, such as seismic sources, instrumental and historical catalogs, M_{min} , M_{max} , and b -value for each defined zone or fault. The second step entails generating catalogs using the Monte Carlo technique and applying the correlation of ground motions based on Eqs. (5) and (6). In the first column of the second step, the number of simulations of magnitude, location, and depth in each corresponding vector equals the required number of earthquakes determined with respect to the rate of earthquake occurrence in each source and considered time interval for seismic catalog generation [T_{tot} in

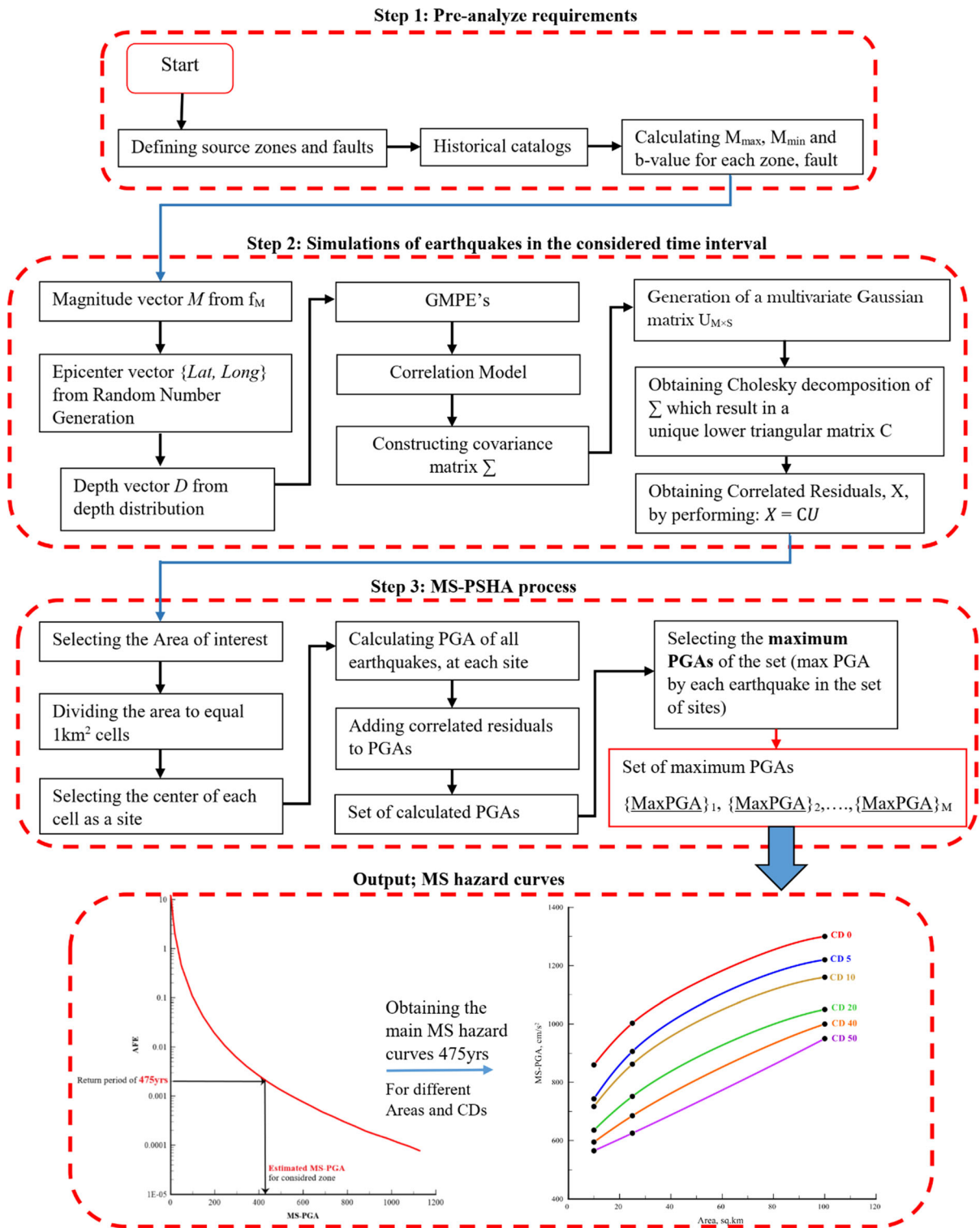


Figure 1
MS-PSHA implementation flowchart

Eq. (7)]. This column could be repeated to obtain the desired number of catalogs. M and S in the second step's last column represent the number of simulated earthquakes and considered sites, respectively. The final step is the calculation of MS hazard curves based on the statistical concept mentioned earlier. This step includes selecting the interested area, dividing it into equal cells, computing produced ground motion parameters at the center of each cell as a site, estimating annual exceedance rates of proposed levels in at least one site using Eq. (7), and obtaining MS hazard curves for different CD s and area sizes.

3. The Studied Area and Input Parameters

MS-PSHA must be used in all the cases where the exceedance rate (or probability) in at least one site or multiple sites is required, such as regional seismic hazard analysis or seismic hazard validation studies. In this study, in which we use MS-PSHA as a regional seismic hazard assessment tool, we also attempted to evaluate the performance of MS-PSHA results against recently recorded large earthquakes. It should be noted that the aim of the presented evaluation is emphasizing the necessity of using MS-PSHA in the earlier mentioned cases. Furthermore, this comparison, which involves real data, helps us to trust more in our methodology and analysis to use it in future projects. For this, we should first choose an epicentral area with a high density of recorded strong ground motions, where single-site seismic hazard estimates were frequently exceeded when compared to the observed ground motion values. Sarpol-e

Zahab City in Kermanshah Province, western Iran, is selected as an appropriate area in this study to implement MS-PSHA and examine its performance. This area is located along the Iran–Iraq border and is close to the convergent boundary of the Arabian and Eurasian tectonic plates, as well as the High Zagros Fault and the Mountain Front Fault (Yaghmaei-Sabegh, 2019).

In recent years, this area has been hit by several large destructive earthquakes with all epicenters less than 40 km away. Table 1 provides the characteristics of these earthquakes. As presented, the recorded PGAs differ significantly from design PGAs adopted from Standard No. 2800 (2014). The objective of this comparison is not to justify an outcome of single-site PSHA, as it requires a long time interval and a large number of records. The aim here is to report the observations and emphasize that the selected area corresponds with the mentioned features and is appropriate to investigate MS-PSHA performance.

Seismic source zones for the study area are illustrated in Fig. 2 (adopted from Zafarani et al., 2020). These sources are defined according to the spatial distribution of shallow earthquakes. Moreover, the defined faults are major and thrust faults. Table 2 provides the M_{\max} and b -value of each of the nine source zones (Zafarani et al., 2020) used as input parameters to generate a catalog based on the Monte Carlo technique. The main characteristics of two local and regional GMPEs are reported in Table 3. Notably, the two relationships used in this paper are based on data from crustal earthquakes in Iran and Turkey. We considered PGA as the intensity measure in all sites in our analysis. Figure 3 illustrates an example of a simulated catalog based on the Monte

Table 1

Recently recorded earthquakes in the station of Sarpol-e Zahab City. Design PGA is 300 cm/s²

Number of the earthquake	Date	M_w	Recorded PGA (cm/s ²)	Distance from the city (km)	Ratio recorded PGA/design base acceleration (PGA)
1	12-11-2017	7.3	690	39	2.3
2	01-04-2018	5.3	428	13	1.43
3	25-11-2018	6.4	410	23	1.37

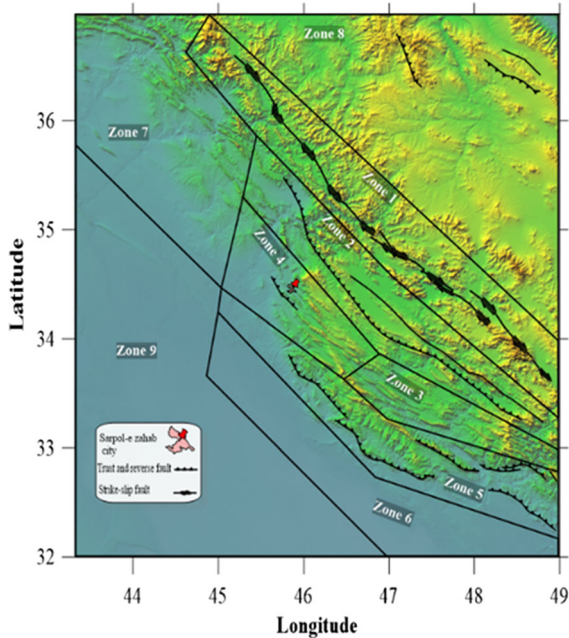


Figure 2
Impactful source zones and faults in Sarpol-e Zahab City (Zafarani et al., 2020)

Table 2

Seismicity parameters of each source zone (Zafarani et al., 2020)

Zone	<i>b</i> -value	<i>M</i> _{max}
1	0.938	7.5
2	0.816	7.5
3	0.612	7.5
4	0.638	7.5
5	0.617	7.5
6	0.798	7.5
7	0.521	7.5
8	1.003	7.9
9	0.651	6.5

Table 3

Selected GMPEs and their characteristics

Number	GMPE	Area	<i>M</i> _{min} - <i>M</i> _{max}	<i>R</i> _{min} - <i>R</i> _{max} (km)
1	Zafarani et al. (2018)	Iran	4_7.3	0 ≤ <i>R</i> _{JB} ≤ 200
2	Kale et al. (2015)	Iran and Turkey	4_8	0 ≤ <i>R</i> _{JB} ≤ 200

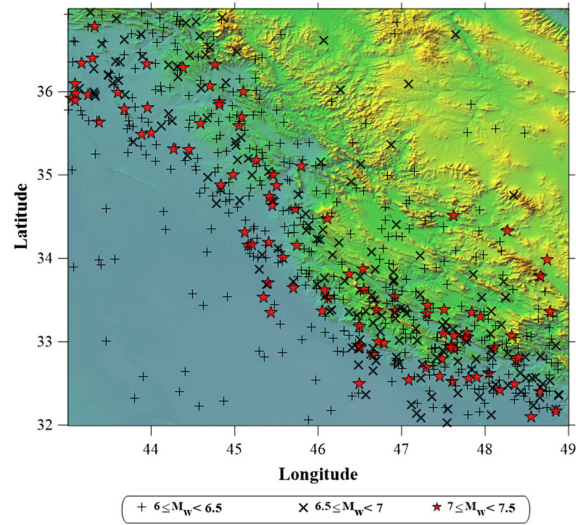


Figure 3
An example of a simulated catalog

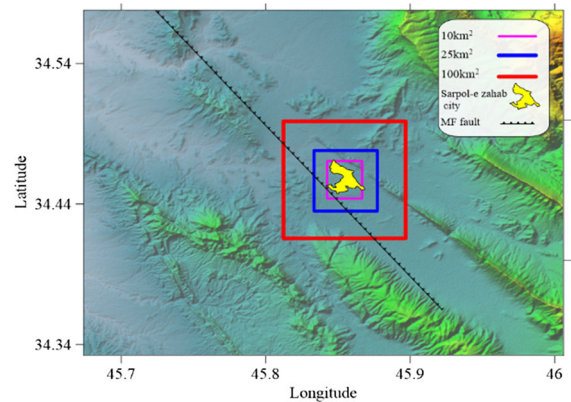


Figure 4
Considered zones for MS-PSHA

Carlo technique, which serves as the primary input for MS-PSHA.

We performed MS-PSHA for three square zones with the areas of 10, 25, and 100 km² which are shown in Fig. 4. The 10 km² zone almost surrounds Sarpol-e Zahab City. Each of these zones is divided into 1 km² cells, and the center of each is considered as a site. Therefore, 10, 25, and 100 km² zones comprise 9, 25, and 100 sites, respectively.

Regardless of the between-earthquake correlation due to its minor effect, five CD_s are considered in this study: 0, 5, 10, 20, 40, and 50 km, referred to as CD₀, CD₅, CD₁₀, CD₂₀, CD₄₀, and CD₅₀, each

representing different within-earthquake correlations. Because ground motion variability increases significantly, the uncorrelated ground motion case ($CD = 0$ km) is unlikely and is only considered for comparison. Furthermore, the case of $CD = 50$ km is regarded as having the highest level of correlation, implying a linear distribution of ground motion in sites. The adopted exponential correlation model is the developed local one in the Zafarani et al. study (2020) (see Fig. 7).

4. Results of MS-PSHA

To show the dependence of results on zone size and CD level, we present the implemented MS-PSHA results, herein in terms of PGA, for three zones with areas of 10, 25, and 100 km² and five CD s of 50, 40, 20, 10, 5, 0 km. Larger zone sizes and smaller CD s result in higher hazard estimates (see Fig. 5). According to Fig. 5, the minimum MS-PGA is 549.6 cm/s² if the zone size is minimum (10 km²) and the CD is maximum (50 km), and the maximum MS-PGA is 1212 cm/s² if the zone size is maximum (100 km²) and the CD is minimum (0 km). Taking all five CD s into account, the average increase of MS-PGA from 10 to 25 km², 10 to 100 km², and 25 to 100

km² is 16.5%, 44.3%, and 23.9%, respectively. When all three sizes are considered, the difference between estimated MS-PGAs for 10 and 20 km CD s is higher than for other CD s (Fig. 5). Figure 4 shows the zones considered in MS-PSHA given the location of Sarpol-e Zahab City.

The variation of MS-PGA estimates against CD s is shown in Fig. 6, demonstrating that by increasing the CD when the zone size is fixed, the MS-PGA decreases. On the other hand, by increasing the zone size when the CD is fixed, the MS-PGA value increases. Considering all three zone sizes, the average decrease of MS-PGA when the CD increases from 5 to 10 km is about 5.4% (the lowest decrease), and from 0 to 50 km is 37.2% (the highest decrease). According to this figure, the slope of the graph becomes steeper when the CD is increased from 10 to 20 km, indicating a significant difference between these two distances rather than others.

To evaluate the performance of MS-PSHA, we compared the results with the recorded PGAs of recent earthquakes in Sarpol-e Zahab City (see Table 1). First, the correlation function should be selected, which is adopted from Zafarani et al.'s study (2020) in this paper. Using Fig. 7 and drawing the CD line ($\rho_\varepsilon = 0.368$), the CD for the study case equals 9.89 km, a reasonable approximation of

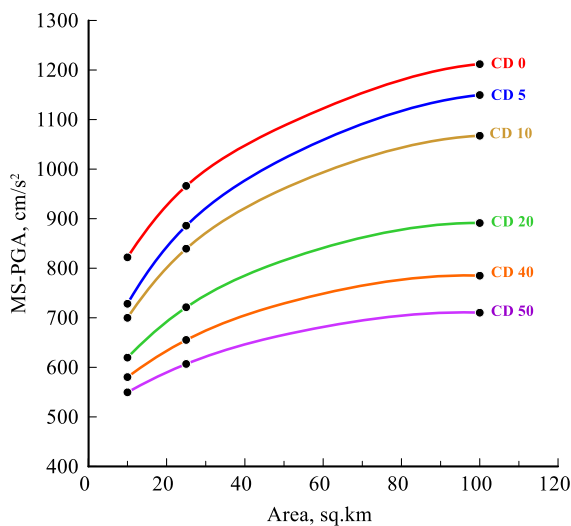


Figure 5

MS hazard curves with a return period of 475 years. Solid circles show individual MS-PGAs, and MS hazard curves are obtained by spline interpolation

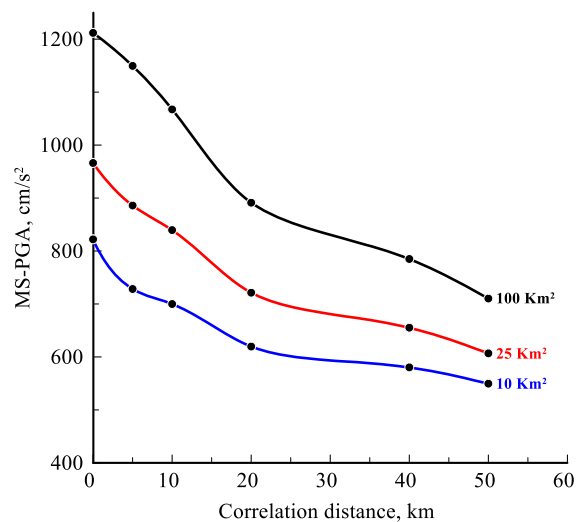


Figure 6

Dependence of MS-PGAs with a return period of 475 years on CD . Solid circles show individual MS-PGAs, and MS hazard curves are obtained by spline interpolation

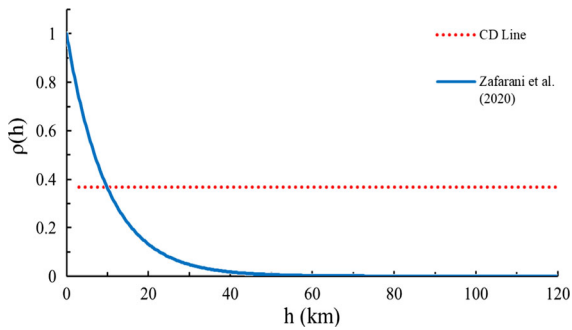


Figure 7
Estimate of CD for the considered zone

10 km. Therefore, as a result of MS hazard curves presented in Fig. 5, the MS-PGA for the Sarpol-e Zahab City, which is approximately located in a 10 km² square, is 700 cm/s². According to Fig. 8, which combines MS hazard curves and recorded PGAs, the estimated MS-PGA for Sarpol-e Zahab City is higher than all recorded PGAs in this city. The maximum recorded PGA in the city (690 cm/s²) is higher than the MS-PGAs estimated for areas less than 20, 34, and 63 km² with CD_s of 20, 40, and

50 km, respectively, according to Fig. 8. Note that the return period of earthquake #1 in Table 1 is 1010 years.

It is important to point out that the considered earthquakes for the preliminary analysis of MS-PSHA performance contain the following features: (1) being located near the study area, (2) the recorded ground motions exceeded design ground motions, and (3) caused extensive life and financial losses, which help us to achieve our mentioned goals in Sect. 3. While the number of earthquakes with mentioned features is small, this comparison could still be an appropriate examination as these records are the highest ones in almost the last 30 years, recorded in the seismic station of this city.

So far, MS-PSHA has been implemented in the Sarpol-e Zahab area, considering different CD_s and zone sizes, and its outcomes in terms of PGA have been compared to recently recorded earthquakes. One may argue how officials and engineers can use this analysis to evaluate current design codes and adopt new approaches to design structures. Therefore, in the

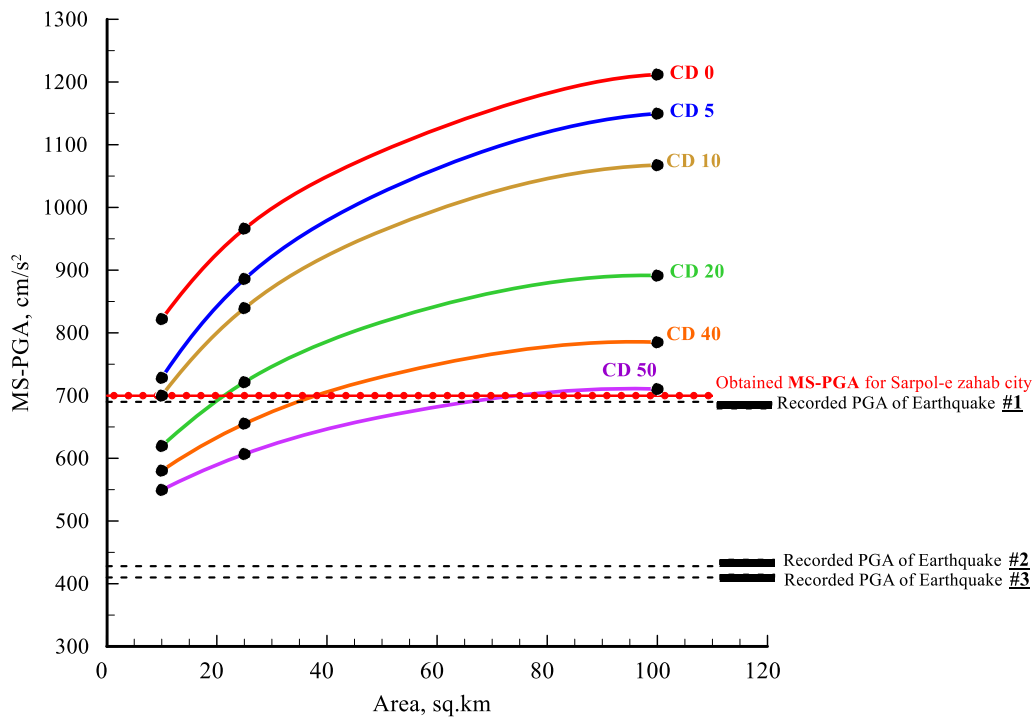


Figure 8
MS hazard curves and recorded PGAs in Sarpol-e Zahab City. The red line shows the estimated MS-PGA for Sarpol-e Zahab City

next section, two proposals are represented in this context, providing corresponding outcomes based on Sarpol-e Zahab City.

5. *Proposals on the Use of MS-PSHA*

5.1. *Evaluating Design Ground Motion Based on MS-PSHA*

A specific ground motion level with a particular return period or an exceedance probability in a time interval would be selected based on single-site PSHA regarding different objectives. A ground motion level with a 10% probability of exceedance in 50 years is widely adopted as design ground motion (DM), and the corresponding earthquake as design-based earthquake (DBE), in building codes (Standard No. 2800, 2014; European Committee for Standardization, 2004). Based on single-site PSHA principles, the exceedance probability of DM is estimated for a single site, while it would be increased in the case of considering DM exceedance probability in at least one site of several in a city or particular zone (Iervolino, 2013). It would be understandable, as it is much more likely that at least one person is affected by COVID-19 in a city rather than only an individual. Therefore, it seems necessary to consider this probability in adopting and defining DM to increase social safety and obtain wider perspectives on potential consequences. While one may question this consideration because of increased DM computed by means of single-site PSHA, it should be noted that there are cases in which it is useful and even necessary to define DM based on MS-PSHA estimates. One of the cases is when the destruction of at least one element of a distributed structure can stop the operation or cause a social disaster and affect a wide area. Examples could be the destruction of gas and water supply stations, hospitals, and nuclear stations. Another case is when the exceedance probability of DM, computed by means of single-site PSHA, in at least one site, in the considered region, is high. Here, a DM with lower exceedance probabilities in at least one site could be adopted to avoid possible damages that are discussed in the following paragraph.

Before discussing the effect of this probability on DM defining, it may be helpful first to explain the concepts of MS-PSHA estimates. As the term “at least one site” is used in MS-PSHA, the maximum ground motions among the sites are used to estimate exceedance rates from intensity levels. As a result, the estimated exceedance rates or probabilities of considered intensity levels are the highest in a given time interval. This feature allows us to make comprehensive and informed decisions about proper DM. As an example, if we adopt DM as 0.3 g (PGA) (Standard No. 2800), according to the MS hazard curve derived for Sarpol-e Zahab City considering *CD10*, the probability of exceeding DM in the next 50 years in at least one of the sites in the city is 65%. As is obvious, it is highly likely to be exceeded in at least one of the sites, each of which corresponds to a 1 km² neighborhood. This may warn us about probable damages that are mostly socially affecting ones like the destruction of crucial structures, located at two or more sites, and access ban due to destruction jams in more than one site. As a more tangible example, imagine a region divided into nine sites each corresponding to a 1 km area, and four crucial structures are distributed in these nine sites, or a gas or water supply network is distributed over four sites. A high probability of exceeding DM, in which these structures are constructed or will be constructed, in at least one site of this region is a warning of destruction or failure in operation that will affect a wide area.

Considering the following questions could possibly guide us through selecting proper DM involving MS-PSHA estimates: (1) Is it possible to provide post-earthquake relief despite the damages and collapses in at least one area of the city? (2) Is there at least one area in the city where critical elements of lifelines are concentrated?

Positive answers to these questions may indicate the importance of considering the exceedance probability of DM in at least one site and taking advantage of MS-PSHA estimations in designing lifelines, as their destruction in at least one site causes serious consequences. Depending on officials' risk management policies, it is also possible to define a reference probability of exceedance in at least one site as a safe or acceptable level.

5.2. Defining the Maximum Considered Earthquake (MCE) and the Collapse Prevention Level Based on MS-PSHA Estimates

Based on single-site PSHA results, a ground motion level with an exceedance probability of 2% in 50 years is adopted as the collapse prevention level, and the corresponding earthquake as MCE. The goal of defining this level is to prevent the collapse of a structure in the event of large and low-probability earthquakes in which ground motions exceed DM. In fact, it provides an extra capability for structures to withstand collapse. In many earthquakes, as mentioned in Tsang (2011), and the 2017 Sarpol-e Zahab earthquake, collapse prevention levels were significantly exceeded in epicentral areas. Taking this into account, instead of adopting ground motion levels with lower probabilities, for example, 0.5% in 50 years, MS-PSHA can provide alternative approaches (Sokolov & Ismail-Zadeh, 2016). Based on MS-PSHA estimates, a ground motion level with a specific probability, for example, 10%, of exceedance in at least one site could be introduced as the collapse prevention level and MCE. This choice can have two main advantages: (1) adopting ground motion levels with a low probability of exceedance is associated with uncertainty, as large, rare, and low-probability earthquakes play an important role in their estimation. As we know, considering these earthquakes is difficult in most cases due to limited sources, especially in areas with rare and limited seismic data. Therefore, higher exceedance probabilities resulting from MS-PSHA can help to reduce this uncertainty to some extent. (2) The collapse of a building can result in secondary damages and even a social crisis in the case of a lifeline element collapse. Therefore, adopting a ground motion with a specific probability of exceedance in at least one site over a given time interval would allow us to consider the social risk aspect when defining the collapse prevention level.

If we select the MCE ground motion and collapse prevention level based on the proposed approach and adopt DM based on single-site PSHA as the ground motion with a 10% probability of exceedance in 50 years, an issue arises due to the difference between these levels, decreasing building safety

against collapse. For instance, for Sarpol-e Zahab City, based on single-site PSHA and Standard No. 2800, DM with a 475-year return period equals 0.3 g (PGA), and based on MS-PSHA and considering *CD10*, MCE ground motion or collapse prevention level with a 475-year return period equals 0.7 g (PGA). This significant difference (MCE/DBE = 2.33) indicates that the designed structure will probably not survive the MCE ground motion. To overcome this issue, a seismic margin of 1.5 could be used to increase safety against collapse. Therefore, multiplying 2/3 by MCE ground motions yields DM or DBE ground motions. This value for Sarpol-e Zahab City equals 0.46 g. It should be noted that adopting ground motions with different probabilities of exceedance in at least one site as the MCE level is directly dependent on the structure's importance level and design life, as discussed in Sect. 6.2.

In the next section, two extended examples based on Sarpol-e Zahab City are provided.

6. Engineering Applications of Represented Proposals

6.1. MS Design Spectrum for Sarpol-e Zahab City and Evaluation of the Iranian Code Design Spectrum

In Sect. 5.1, it was proposed that MS-PSHA estimates could be used to evaluate DM and generally single-site PSHA outcomes such as design spectrum. It was also discussed that MS estimates could be used as a basis to design crucial and lifeline structures. Therefore, in this section, based on these proposals, MS design spectra are developed for the 10 km² Sarpol-e Zahab zone (Fig. 4), with different probabilities of exceedance in at least one site in 50 years, and the Iranian code design spectrum (based on Standard No. 2800) is discussed in the light of developed MS design spectra. It should be noted that the Iranian code design spectrum (assumed rock condition) is multiplied by an importance factor of 1.4, as reported by Standard No. 2800 for "very important" structures. The *CD10* is used to develop MS design spectra since it is the exact value for the study area based on Sect. 4 and provides meaningful

comparisons. The following are the objectives of discussing the code design spectrum based on MS design spectra:

- (1) To determine the difference between the adopted DM based on the MS design spectrum and the corresponding value based on the code design spectrum, and the amount of change in this difference if a higher probability of exceedance in at least one site is selected
- (2) Investigation of the code design spectrum probability of exceedance in at least one site at different periods and identifying periods with a high probability of exceedance. In other words, determining the associated hazard of exceeding in at least one site with selected DM based on the code design spectrum.

As shown in Fig. 9, spectral accelerations (SA) with natural periods shorter than 0.22 s have the highest probability of exceedance in at least one site and reach almost 50% at period 0.15 s and some lower periods. On the other hand, for those with natural periods longer than 1.7 s, this probability is lower than 10%. The maximum SA (g) occurred at $T = 0.15$ s in all assumed probabilities of exceedance in MS design spectra. The difference between the MS

design spectrum with 475-year return period and the code design spectrum decreases significantly at a natural period of 0.4 s, and this difference decreases further as the natural period increases, reaching zero at $T = 1.7$ s. The MS design spectra decrease at short periods by selecting higher probabilities of exceedance and, consequently, accepting higher hazards. It is important to note that as the occurrence of earthquakes in each of the sources follows a homogeneous Poisson process (HPP), the earthquakes causing exceedance in at least one site also occur according to an HPP (called filtered or thinned Poisson process; Giorgio & Iervolino, 2016). Therefore, expressing MS-PSHA estimates in terms of return period and comparison of them with the code design spectrum is meaningful.

As a conclusion, comparing the MS design spectra with the code design spectrum (developed based on single-site PSHA) shows that in the case of selecting DM from the code design spectrum for designing very important short-story structures (with short natural periods) in the city of Sarpol-e Zahab, there is a high probability of exceeding selected DM in at least one sites of several in the city (each site is representative of a 1 km² neighborhood). This high probability may warn us about a possible social crisis

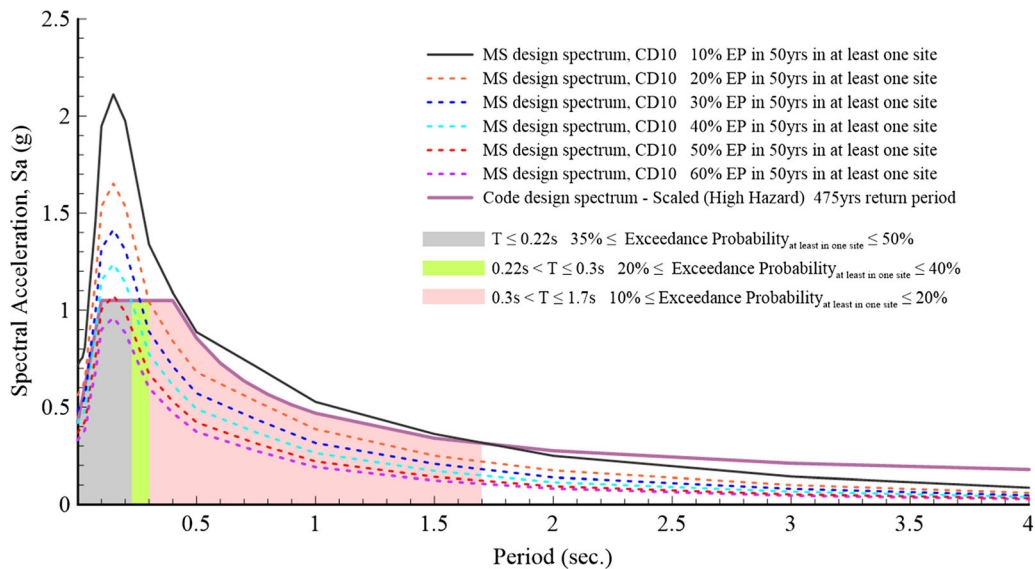


Figure 9

MS design spectra with different probabilities of exceedance in at least one site and their comparison with the code design spectrum (rock site) for very high-importance structures

due to probable damages to a very important structure in the next 50 years.

To further examine the MS design spectrum, the response spectrum of the Sarpol-e Zahab 2017 earthquake is compared with the MS design spectrum with a 10% probability of exceedance in at least one site (Fig. 10). It should be noted that this is a preliminary performance evolution rather than an absolute validation of the MS design spectrum. According to Fig. 10, the MS design spectrum represents reasonable estimates of SA at natural periods in which the response is maximum (0.22 s and 0.28 s) and also at shorter periods.

Moreover, the code design spectrum was significantly exceeded at short periods. It could be expected, as, with respect to Fig. 9, the probability of exceeding SA in at least one site at natural periods less than 0.28 (the second highest SA) is between 20 and 50%, which increases at lower periods.

6.2. Using MS-PSHA Estimates to Adopt MCE Ground Motions and Develop DBE-level Uniform Hazard Spectra

In Sect. 5.2, it was proposed that MS-PSHA estimates could be introduced as MCE ground motions and collapse prevention levels. Multiplying

the resultant MCE ground motions by 2/3 will provide DBE ground motions, and then based on these ground motions, the DBE-level uniform hazard spectrum (UHS) could be provided.

In this regard, two different cases of MS uniform hazard spectra are selected as MCE ground motions: (1) MS uniform hazard spectra based on CD_{10} and three different probabilities of exceedance in at least one site (10%, 20%, and 30%) in 50 years; and (2) MS uniform hazard spectra based on 10% probability of exceedance in at least one site in 50 years and three different CD s (10 km, 20 km, and 40 km). Both of these cases are applied to the 10 km² Sarpol-e Zahab zone (Fig. 4). As a result of these selections, MCE and DBE ground motions could be selected based on both different exceedance probabilities (different hazards) and different CD s (different variability). In selecting these two levels, case (1) allows us to be flexible in considering structures with different importance levels by defining different hazard levels based on given exceedance probabilities, while case (2) enables us to consider recorded earthquake features and local site effects.

To further explain, these spectra could be used to design structures, rather than those of very high importance, the collapse of which could also cause extensive life and financial losses. Such structures

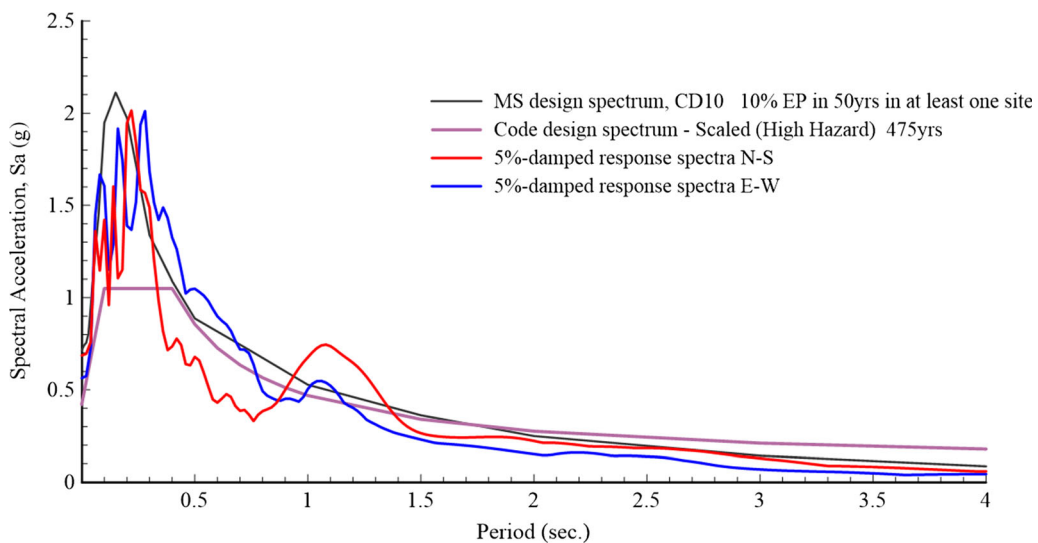


Figure 10
Comparison of the MS design spectrum with two components of the 2017 Sarpol-e Zahab earthquake

may include large residential complexes, the destruction of which causes secondary damages and significant loss of life. In more detail, different exceedance probabilities in at least one site and *CDs* could be used regarding the importance of a structure and possible secondary damages in the case of exceeding DM or collapse. Higher probabilities of exceedance in at least one site, for example, may be used for structures whose destruction does not cause significant secondary damages or a possible social crisis. In Figs. 11 and 12, DBE-level uniform hazard spectra based on defined cases (1) and (2) are plotted along with the code design spectrum (on rock and for ordinary buildings), respectively.

According to Figs. 11 and 12, by increasing the exceedance probability and *CD*, as expected, DBE-level uniform hazard spectra decrease and approach the code design spectrum, though the differences at short periods remain. In the case of adopting DM from the code design spectrum, to compensate for this difference at short periods, one possible solution is to increase the given hazard level of this zone from “high hazard” to “very high hazard,” according to Standard No. 2800. The result of this suggestion is shown in Figs. 13 and 14.

To further analyze the performance of provided DBE-level UHS for defined cases, we compared them to the response spectrum of the Sarpol-e Zahab 2017 earthquake. The main purpose of this comparison is to assess the level of safety against collapse in the event of an epicentral and large earthquake with a longer return period (1010 years) than that of the MEC level. For this aim, code-type smooth response design spectra were developed based on Malhotra (2006) for each DBE-level UHS. The smooth response design spectra are computed as follows.

First, the control period T_s is computed as

$$T_s = \frac{SA(1s)}{SA(0.2s)} \cdot 1s. \tag{8}$$

Then, the response design spectrum is computed from

$$\begin{cases} 0.4 \cdot SA(0.2s) + 3.0 \cdot SA(0.2s) \cdot \frac{T}{T_s} & T \leq 0.2 \cdot T_s \\ SA(T) = SA(0.2s) & 0.2 \cdot T_s < T < T_s \\ SA(1s) \cdot \frac{T}{T_s} & T > T_s \end{cases} \tag{9}$$

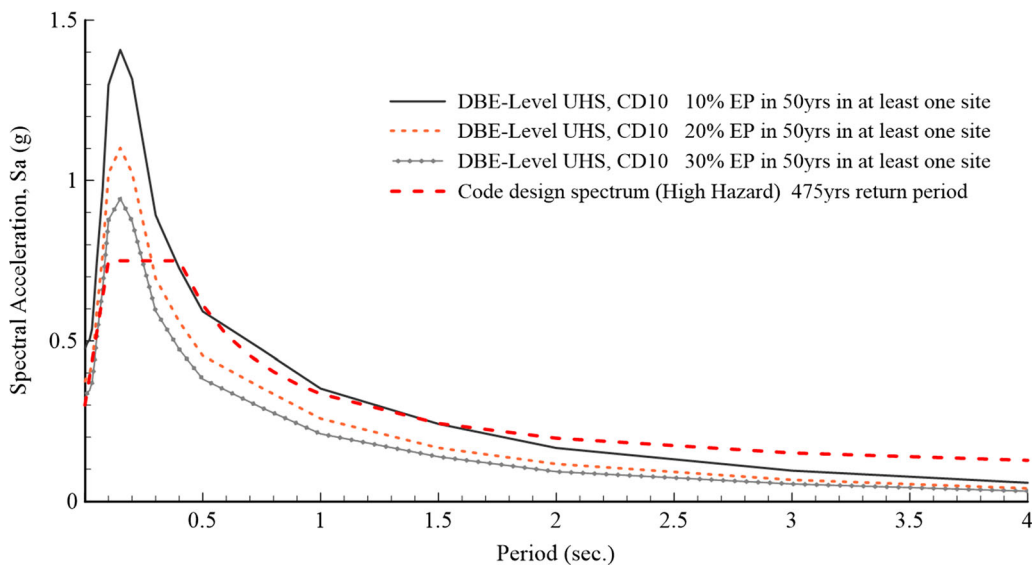


Figure 11 DBE-level uniform hazard spectra for three different exceedance probabilities and the code design spectrum considering high hazard level

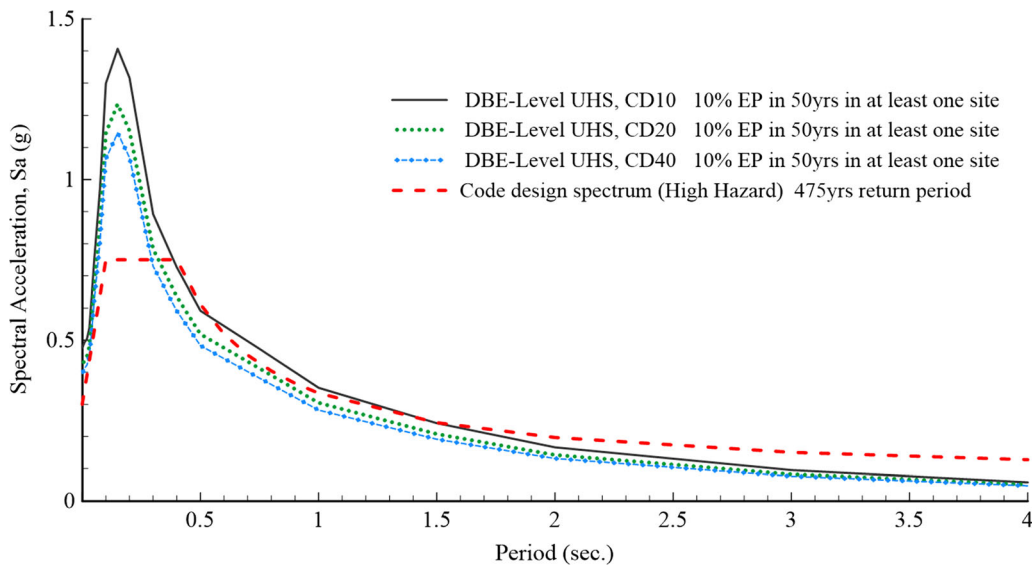


Figure 12

DBE-level uniform hazard spectra for three different CDs and the code design spectrum considering high hazard level

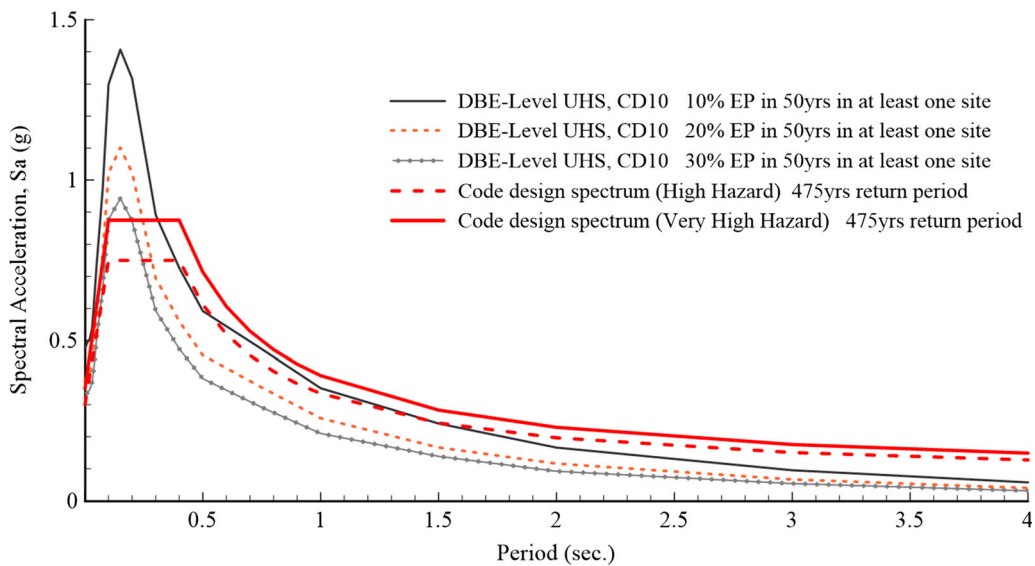


Figure 13

DBE-level uniform hazard spectra for different exceedance probabilities and the code design spectrum considering very high hazard level

These DBE-level code-type design spectra are plotted together in Fig. 15. The provided mean margins, considering all periods, with respect to earthquake response are 1.03, 1.19, 1.28, 1.4, and 1.7

for DBE-level response spectra of *CD10*, *CD20*, and *CD40* with 10%, and *CD10* with 20% and 30% (probabilities of exceedance in at least one site in 50 years), respectively.

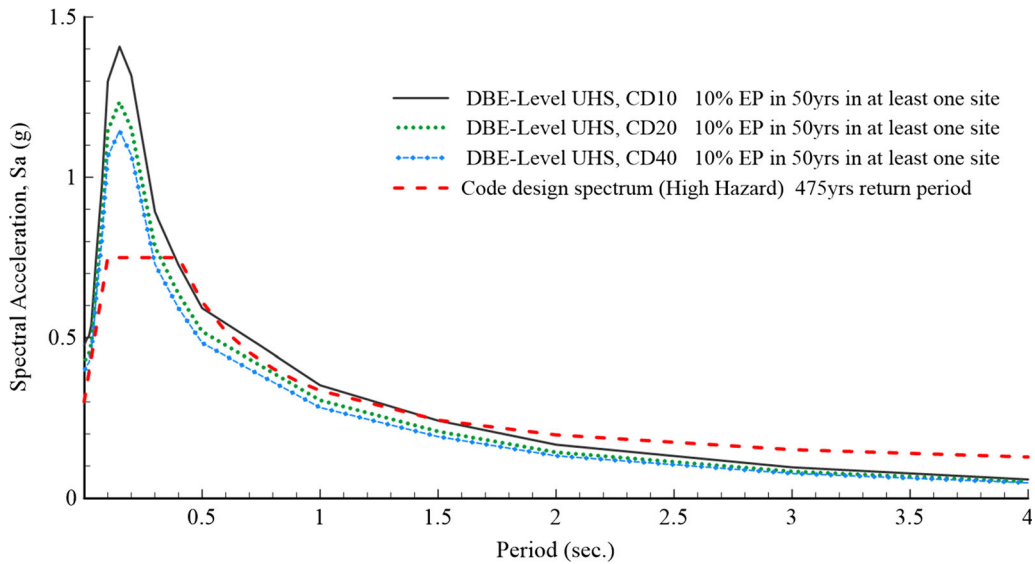


Figure 14

DBE-level uniform hazard spectra for three different CDs and the code design spectrum considering very high hazard level

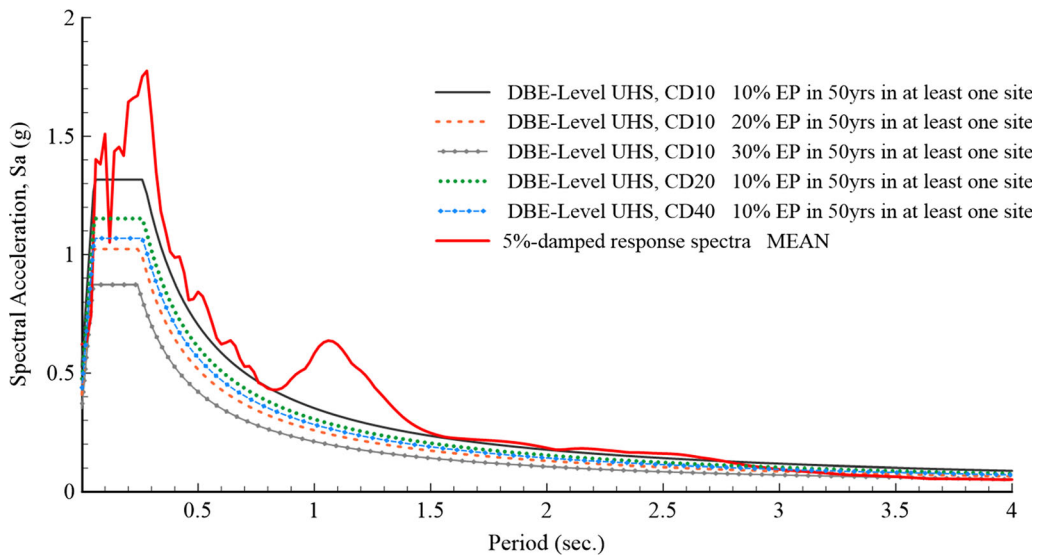


Figure 15

MS code-type smooth response design spectra based on Malhotra (2006) and the mean response spectrum of the 2017 Sarpol-e Zahab earthquake

7. A Short Note About Correlation Distance (CD)

As explained, *CD* is associated with the variability of an earthquake's ground motion in different sites. A small *CD* indicates high variability, while a large one indicates low variability.

Although it is evident that the most reliable approach is to develop the local spatial correlation model and use the exact local value for *CD*, when defining various seismic scenarios and encountering limited data, it is possible to use *CD*10 (high variability) and lower values to define the worst or

the most critical scenarios, as low-probability events play a crucial role in hazard estimation in these cases. The reason is the high variability in these correlation distances. Assuming CD_{10} , the total correlation coefficient between two sites at a distance of 2 km from each other in the study area equals 0.64, indicating high variability of ground motions between two sites located closely. Therefore, these could be used to determine the highest risk of damage, collapse, and exceeding the desired level of ground motion. The corresponding estimated total correlation coefficient for CD_{20} (mid-variability) and CD_{40} (low variability) are 0.84 and 0.91, respectively. Thus, larger CD s, e.g., CD_{20} and CD_{40} , could be used to determine more probable and less conservative scenarios.

8. Conclusion

MS-PSHA could be employed to design lifelines, critical structures, extended buildings, and even ordinary structures with significant collapse consequences. This study attempted to implement MS-PSHA in Sarpol-e Zahab City and define two possible proposals on the use of MS-PSHA. The proposals were applied to a region where the code design spectrum is prone to be exceeded largely in the event of a low-probability event. The key findings are as follows:

- The MS design spectrum, derived for the 10 km² Sarpol-e Zahab zone considering rock condition, with a 10% probability of exceedance in at least one site, is largely compatible with the 2017 Sarpol-e Zahab earthquake response spectra (recorded on rock), especially at periods where the response is maximum.
- In the light of MS-PSHA, the evaluation of the code design spectrum exceedance probability in at least one site could be reliable, as its exceedance at short periods (Fig. 10) in at least one site was expected based on Fig. 9.
- Code-based structures constructed on rock with natural periods less than 0.3 s have a moderate to high probability of exceedance in at least one site over the city of Sarpol-e Zahab.

- Adopting DBE-level uniform hazard spectra based on MS-PSHA estimates provided adequate safety against collapse compared to the 2017 Sarpol-e Zahab earthquake as a low-probability event.
- In the case of designing high-importance structures in Sarpol-e Zahab City based on the Iranian code design spectrum, it is recommended to increase the prescribed seismic hazard level for this city from “high hazard” to “very high hazard.”
- Based on DBE-level uniform hazard spectra, various design strategies could be adopted with respect to different CD s and probabilities of exceedance in at least one site.

In conclusion, it is crucial to point out that the current study did not attempt to convey the message that single-site PSHA was unable to properly assess the seismic hazard in the study area, but rather tried to implement MS-PSHA as a regional seismic hazard assessment tool to widen our assumed seismic hazard perception about possible scenarios that could significantly damage the entire study area, as happened in the 2017 Sarpol-e Zahab event, and to propose and define flexible alternative and complementary seismic actions to survive these extreme and low-probability events. Future studies could integrate characteristics such as near-field ground motions, local site effects, and characteristic earthquake effects into the MS-PSHA.

Funding

There is not any funding for this study.

Declarations

Conflict of Interest The authors declare that there is no conflict of interest.

Publisher’s Note Springer Nature remains neutral with regard to jurisdictional claims in published maps and institutional affiliations.

Springer Nature or its licensor holds exclusive rights to this article under a publishing agreement with the author(s) or other rightsholder(s); author self-archiving of the accepted manuscript version of this article

is solely governed by the terms of such publishing agreement and applicable law.

REFERENCES

- Albarelo, D., & D'amico, V. (2008). Testing probabilistic seismic hazard estimates by comparison with observations: An example in Italy. *Geophysical Journal International*, 175(3), 1088–1094. <https://doi.org/10.1111/j.1365-246X.2008.03928.x>
- Anderson, J. G., & Biasi, G. P. (2016). What is the basic assumption for probabilistic seismic hazard assessment? *Seismological Research Letters*, 87(2A), 323–326. <https://doi.org/10.1785/0220150232>
- Assatourians, K., & Atkinson, G. M. (2013). EqHaz: An open-source probabilistic seismic-hazard code based on the Monte Carlo simulation approach. *Seismological Research Letters*, 84(3), 516–524. <https://doi.org/10.1785/0220120102>
- Bourne, S. J., Oates, S. J., Bommer, J. J., Dost, B., Van Elk, J., & Doornhof, D. (2015). A monte carlo method for probabilistic hazard assessment of induced seismicity due to conventional natural gas production. *Bulletin of the Seismological Society of America*, 105(3), 1721–1738. <https://doi.org/10.1785/0120140302>
- Building and Housing Research Center (BHRC). (2014). *Iranian code of practice for seismic resistant design of buildings (standard no. 2800)*. Building and Housing Research Center (BHRC).
- Chioccarelli, E., Cito, P., Iervolino, I., & Giorgio, M. (2019). REASSESS V2.0: Software for single- and multi-site probabilistic seismic hazard analysis. *Bulletin of Earthquake Engineering*, 17, 1769–1793.
- Cornell, C. A. (1968). Engineering seismic risk analysis. *Bulletin of the Seismological Society of America*, 58(5), 1583–1606. <https://doi.org/10.1785/BSSA0580051583>
- Ebel, J. E., & Kafka, A. L. (1999). A Monte Carlo approach to seismic hazard analysis. *Bulletin of the Seismological Society of America*, 89(4), 854–866. <https://doi.org/10.1785/BSSA0890040854>
- Esposito, S., & Iervolino, I. (2012). Spatial correlation of spectral acceleration in European data. *Bulletin of the Seismological Society of America*, 102(6), 2781–2788. <https://doi.org/10.1785/0120120068>
- European Committee for Standardization. (2004). Eurocode 8: Design of structures for earthquake resistance - Part 1: General rules, seismic actions and rules for buildings. *European Committee for Standardization*, 1(English).
- Frankel, A. (2013). Comment on “Why earthquake hazard maps often fail and what to do about it” by S. Stein, R. Geller, and M. Liu. *Tectonophysics*, 592, 200–206. <https://doi.org/10.1016/j.tecto.2012.11.032>
- Geller, R. J. (2011). Shake-up time for Japanese seismology. *Nature*, 472(7344), 407–409. <https://doi.org/10.1038/nature10105>
- Giorgio, M., & Iervolino, I. (2016). On multisite probabilistic seismic hazard analysis. *Bulletin of the Seismological Society of America*, 106(3), 1223–1234. <https://doi.org/10.1785/0120150369>
- Goda, K., & Hong, H. P. (2008). Spatial correlation of peak ground motions and response spectra. *Bulletin of the Seismological Society of America*, 98(1), 354–365. <https://doi.org/10.1785/0120070078>
- Hanks, T. C., Beroza, G. C., & Toda, S. (2012). Have recent earthquakes exposed flaws in or misunderstandings of probabilistic seismic hazard analysis? *Seismological Research Letters*, 83(5), 759–764. <https://doi.org/10.1785/0220120043>
- Iervolino, I. (2013). Probabilities and fallacies: Why hazard maps cannot be validated by individual earthquakes. *Earthquake Spectra*, 29(3), 1125–1136. <https://doi.org/10.1193/1.4000152>
- Iervolino, I., Giorgio, M., & Cito, P. (2017). The effect of spatial dependence on hazard validation. *Geophys Journ Int*, 209, 1363–1368.
- Jayaram, N., & Baker, J. W. (2008). Statistical tests of the joint distribution of spectral acceleration values. *Bulletin of the Seismological Society of America*, 98(5), 2231–2243. <https://doi.org/10.1785/0120070208>
- Jayaram, N., & Baker, J. W. (2009). Correlation model for spatially distributed ground-motion intensities. *Earthquake Engineering and Structural Dynamics*, 38(15), 1687–1708. <https://doi.org/10.1002/eqe.922>
- Kale, Ö., Akkar, S., Ansari, A., & Hamzehloo, H. (2015). A ground-motion predictive model for iran and turkey for horizontal PGA, PGV, and 5% damped response spectrum: Investigation of possible regional effects. *Bulletin of the Seismological Society of America*, 105(2), 963–980. <https://doi.org/10.1785/0120140134>
- Klüge, J. U. (2012). Comment on “earthquake hazard maps and objective testing: The Hazard Mapper’s point of view” by Mark W. Stirling. *Seismological Research Letters*, 83(5), 829–830. <https://doi.org/10.1785/0220120051>
- Kossobokov, V. G., & Nekrasova, A. K. (2012). Global Seismic Hazard Assessment Program maps are erroneous. *Seismic Instruments*, 48(2), 162–170. <https://doi.org/10.3103/s0747923912020065>
- Malhotra, P. K. (2006). Return Period of Recorded Ground Motion. *Journal of Structural Engineering*, 132(6), 833–839. [https://doi.org/10.1061/\(asce\)0773-9445\(2006\)132:6\(833\)](https://doi.org/10.1061/(asce)0773-9445(2006)132:6(833))
- Musson, R. M. W. (1999). Determination of design earthquakes in seismic hazard analysis through monte carlo simulation. *Journal of Earthquake Engineering*, 3(4), 463–474. <https://doi.org/10.1080/13632469909350355>
- Panza, G., Kossobokov, V. G., Peresan, A., & Nekrasova, A. (2014). Why are the Standard Probabilistic Methods of Estimating Seismic Hazard and Risks Too Often Wrong. In *Earthquake Hazard, Risk and Disasters* (pp. 309–357). Elsevier Inc. <https://doi.org/10.1016/B978-0-12-394848-9.00012-2>
- Panza, G. F., Irikura, K., Kouteva, M., Peresan, A., Wang, Z., & Saragoni, R. (2011). Advanced seismic hazard assessment. In *Pure and Applied Geophysics*, 168(1–2), 1–9. <https://doi.org/10.1007/s00024-010-0179-9>
- Park, J., Bazzurro, P., & Baker, J. (2007). Modeling spatial correlation of ground motion Intensity Measures for regional seismic hazard and portfolio loss estimation. *Applications of Statistics and Probability in Civil Engineering - Proceedings of the 10th International Conference on Applications of Statistics and Probability*, ICASP10.
- Rhoades, D. A., & McVerry, G. H. (2001). Joint hazard of earthquake shaking at two or more locations. *Earthquake Spectra*, 17(4), 697–710. <https://doi.org/10.1193/1.1423903>

- Schorlemmer, D., Gerstenberger, M., Wiemer, S., Jackson, D. D., & Rhoades, D. A. (2007). Earthquake likelihood model testing. *Seismological Research Letters*, 78, 17–29.
- Sokolov, V., & Ismail-Zadeh, A. (2016). On the use of multiple-site estimations in probabilistic seismic-hazard assessment. *Bulletin of the Seismological Society of America*, 106(5), 2233–2243. <https://doi.org/10.1785/0120150306>
- Sokolov, V., & Wenzel, F. (2011). Influence of ground-motion correlation on probabilistic assessments of seismic hazard and loss: Sensitivity analysis. *Bulletin of Earthquake Engineering*, 9(5), 1339–1360. <https://doi.org/10.1007/s10518-011-9264-4>
- Sokolov, V., & Wenzel, F. (2015). On the relation between point-wise and multiple-location probabilistic seismic hazard assessments. *Bulletin of Earthquake Engineering*, 13(5), 1281–1301. <https://doi.org/10.1007/s10518-014-9661-6>
- Stein, S., Geller, R., & Liu, M. (2011). Bad assumptions or bad luck: Why earthquake hazard maps need objective testing. *Seismological Research Letters*, 82(5), 623–626. <https://doi.org/10.1785/gssrl.82.5.623>
- Stirling, M. W. (2012). Earthquake hazard maps and objective testing: The hazard mapper's point of view. *Seismological Research Letters*, 83(2), 231–232. <https://doi.org/10.1785/gssrl.83.2.231>
- Tsang, H. H. (2011). Should we design buildings for lower-probability earthquake motion? *Natural Hazards*, 58(3), 853–857. <https://doi.org/10.1007/s11069-011-9802-z>
- Wang, M., & Takada, T. (2005). Macrospatial correlation model of seismic ground motions. *Earthquake Spectra*, 21(4), 1137–1156. <https://doi.org/10.1193/1.2083887>
- Weatherill, G., & Burton, P. W. (2010). An alternative approach to probabilistic seismic hazard analysis in the Aegean region using Monte Carlo simulation. *Tectonophysics*, 492(1–4), 253–278. <https://doi.org/10.1016/j.tecto.2010.06.022>
- Wesson, R. L., & Perkins, D. M. (2001). Spatial correlation of probabilistic earthquake ground motion and loss. *Bulletin of the Seismological Society of America*, 91(6), 1496–1515. <https://doi.org/10.1785/0120000284>
- Wong, I. G. (2014). How big, how bad, how often: Are extreme events accounted for in modern seismic hazard analyses? *Natural Hazards*, 72(3), 1299–1309. <https://doi.org/10.1007/s11069-013-0598-x>
- Wyss, M. (2015). Testing the basic assumption for probabilistic seismic-hazard assessment: 11 Failures. *Seismological Research Letters*, 86(5), 1404–1411. <https://doi.org/10.1785/0220150014>
- Wyss, M., & Rosset, P. (2013). Mapping seismic risk: The current crisis. *Natural Hazards*, 68(1), 49–52. <https://doi.org/10.1007/s11069-012-0256-8>
- Yaghmaei-Sabegh, S. (2019). Interpretations of ground motion records from the 2017 M w 7.3 Ezgeleh earthquake in Iran. *Bulletin of Earthquake Engineering*, 17(1), 55–71. <https://doi.org/10.1007/s10518-018-0453-2>
- Zafarani, H., Jafarian, Y., Eskandarinejad, A., Lashgari, A., Soghrat, M. R., Sharafi, H., Afraz-e Haji-Saraei, M., & Haji-Saraei, M. A. (2020). Seismic hazard analysis and local site effect of the 2017 M w 7.3 Sarpol-e Zahab, Iran, earthquake. *Natural Hazards*, 103(2), 1783–1805. <https://doi.org/10.1007/s11069-020-04054-0>
- Zafarani, H., Luzzi, L., Lanzano, G., & Soghrat, M. R. (2018). Empirical equations for the prediction of PGA and pseudo spectral accelerations using Iranian strong-motion data. *Journal of Seismology*, 22(1), 263–285. <https://doi.org/10.1007/s10950-017-9704-y>
- Zuccolo, E., Vaccari, F., Peresan, A., & Panza, G. F. (2011). Neo-Deterministic and Probabilistic Seismic Hazard Assessments: A Comparison over the Italian Territory. *Pure and Applied Geophysics*, 168(1–2), 69–83. <https://doi.org/10.1007/s00024-010-0151-8>